ISSN: 2959-6386 (Online), Volume 2, Issue 2

Journal of Knowledge Learning and Science Technology

Journal homepage: https://jklst.org/index.php/home

Integration of Artificial Intelligence for Real-Time Fault Detection in Semiconductor Packaging

Monish Katari[1], Selvakumar Venkatasubbu[2], Gowrisankar Krishnamoorthy3

[1]Marvell Semiconductor Inc, USA

[2]New York Technology Partners, USA

[3]HCL America, USA

Abstract

Semiconductor manufacturing involves a complex sequence of unit processes, where even a minor error can disrupt the entire production chain. Present-day manufacturing setups rely on continuous data monitoring of equipment health, wafer measurements, and inspections to identify any abnormalities that could impact the quality and performance of the final chip. The primary aim is fault detection and classification (FDC), for which a range of techniques including statistical analysis and machine learning algorithms are commonly employed. In this study, we introduce an innovative approach utilizing an artificial immune system (AIS), inspired by biological mechanisms, for FDC in semiconductor equipment. The main culprits behind process failures are shifts caused by the aging of parts and modules over time. Our methodology integrates state variable identification (SVID) data, reflecting current equipment conditions, and optical emission spectroscopy (OES) data, capturing plasma process information under faulty scenarios induced by deliberate gas flow rate adjustments in semiconductor fabrication. Our results demonstrate a modeling prediction accuracy of 94.69% when incorporating selected SVID and OES data, and 93.68% accuracy using OES data alone. In conclusion, we suggest the potential application of AIS in semiconductor process decision-making, offering promising avenues for enhancing fault detection in semiconductor equipment.

Keywords: artificial immune system; fault detection; data mining; decision making; semiconductor equipment

Article Information:

Article history: Received: 01/09/2023 Accepted:15/09/2023 Online: 30/09/2023 Published: 30/09/2023

DOI: https://doi.org/10.60087/jklst.vol2.n3.p495

[i] ***Correspondence author: Monish Katari***

Introduction

With the continuous miniaturization of semiconductor devices, semiconductor manufacturing processes have become increasingly intricate. These processes entail hundreds of consecutive steps, often spanning up to two months to yield the final semiconductor chips. The integration of factories has significantly enhanced manufacturing efficiency, incorporating practices such as decreased waste generation, optimized production equipment utilization, and predictive operations. Predictive operations, encompassing predictive maintenance (PdM), virtual metrology (VM) for metrology prediction, and fault detection and classification (FDC), play pivotal roles in supporting reactive operations, thereby reducing costs and enhancing quality [1][2][3][4]. Any anomaly during these processes can potentially compromise the performance and quality of the final chip.

The implementation of a real-time monitoring and diagnosis system, leveraging vast amounts of data, is imperative to prevent deviations in chip performance or potential chip failures due to faulty process steps. Moreover, research in smart manufacturing, addressing big data challenges in domains like quality control, maintenance, and scheduling, is actively ongoing [5][6][7]. However, the complexity and fragmentation of data generated across manufacturing processes, process control operations, metrology, and inspection pose significant challenges in data processing, despite its criticality and widespread utilization in manufacturing operations. Additionally, current database management systems encounter limitations in accessing, analyzing, and extracting insights from the diverse array of manufacturing data sources within the semiconductor industry [8].

Efforts to address these challenges necessitate expertise in subject matter and domain knowledge to extract meaningful data pertinent to the manufacturing processes. The predictive operations process commences with handling extensive data acquired from sensors, equipment, and wafer metrology and inspection, posing challenges such as improving data collection, transfer, storage, computation speeds, and enhancing data quality. Although advancements in edge computing devices and graphics processing units have substantially improved data collection and computation speeds, ensuring data quality remains a persistent challenge, albeit with ongoing improvements in denoising features [9].

Nevertheless, effective decision-making in the semiconductor technology domain hinges on substantial subject matter expertise.

Advanced process control (APC) systems, comprising FDC and run-to-run (R2R) control components, are prevalent in contemporary fabs, leveraging copious amounts of data to achieve finer control and diagnostics of complex processes [11][12]. Sensors facilitating plasma monitoring, crucial to the actual process, have significantly contributed to APC systems, with studies exploring diverse sensors such as RF sensors, optical sensors, and various probes [13][14]. Despite the significance of numerous measurement processes, their time and cost implications have prompted active research in virtual metrology to address these challenges [15][16]. As processes become more refined, even minor equipment condition changes can induce process faults, underscoring the necessity for fault detection technologies in semiconductor processes. FDC models typically comprise three primary stages: feature extraction, feature selection, and classification, employing various modeling and decision-making algorithms [17].

This paper introduces an artificial immune system (AIS), drawing inspiration from biological systems, to facilitate initial decision-making for identification [18]. The AIS algorithm is adept at detecting abnormal process conditions indicative of faults that could impact process outcomes. Interestingly, the inspiration for employing an AIS stemmed from the COVID-19 pandemic, highlighting its versatility in addressing semiconductor process diagnostic challenges. The study utilizes two types of data: equipment state variable identification (SVID) data obtained from etch equipment and optical emission spectroscopy (OES) data containing plasma chemistry information. OES serves as a valuable plasma monitoring sensor, capturing variations in optical emission intensity as a function of reactants and byproducts within the etch chamber, thus providing essential plasma process insights [19]. By establishing and monitoring a system that seamlessly transfers these two data types to a real-time database, the data can be effectively managed and utilized for process monitoring and detecting process shifts.

Related Work:

Traditional semiconductor manufacturing initially relied on statistical process controls for monitoring the production process. However, as the processes evolved to become more intricate and refined, there arose a need for finer precision

and accuracy in process control, leading to the proposal of advanced process control (APC) systems [20][21]. APC facilitates real-time process monitoring and control through sensor-based detection and control of critical process shifts [21]. Studies employing sensor-based APC, such as those controlling critical dimensions (CD) and phase angle in photomask dry-etch processes using RF sensors, or employing in situ plasma monitoring sensors for process diagnosis and endpoint detection in etch processes, have been conducted [22–24].

Fault detection and classification (FDC), a component of APC systems, addresses process faults stemming from changes in equipment condition due to aging. FDC enables real-time detection of equipment abnormalities and root cause identification. For instance, studies have applied modular neural networks to state variable identification (SVID) data to identify faulty equipment components [25]. Other studies have utilized algorithms such as conjugate-based least-square support vector machines and isolation forest algorithms to detect process abnormalities in real-time [26][27]. Additionally, research employing multiple algorithms, such as ensemble algorithms combined with random forest and k-means clustering, followed by evaluation with k-nearest neighbors (KNN) and naive Bayes classifiers, has been conducted [28]. Studies addressing fault detection in high-density plasma-chemical vapor deposition equipment, employing autoencoder-based models, imputation data, and algorithms like KNN, support vector machines, and logistic regression, as well as anomaly detection using time-series data, have also been reported [29][30][31]. Furthermore, research utilizing plasma monitoring sensor data alongside SVID data has progressed, including fault detection using principal component analysis and statistical monitoring chart using optical emission spectroscopy (OES) data [32]. Neural networks have been applied to OES and residual gas analysis data for FDC in reactive ion etching [33]. The field of FDC has witnessed significant advancements in recent years, incorporating diverse data and algorithms.

Algorithm:

The immune system, a biological defense mechanism, safeguards the body by identifying and eliminating foreign substances known as antigens, including viruses, bacteria, and other pathogens. It comprises two defense systems: the innate immune system and the adaptive immune system, primarily maintained by white blood cells. Granulocytes and macrophages, key players in the innate immune system, promptly attack foreign substances indiscriminately.

Conversely, lymphocytes, pivotal to the adaptive immune system, produce antibodies that specifically target antigens, thus conferring immunity upon subsequent encounters [34][35][36].

Artificial immune systems (AISs) are algorithms inspired by the principles of the immune system. Leveraging their classification and reasoning capabilities, AIS algorithms address pattern recognition, optimization, machine learning, and computer network security challenges [36]. These systems predominantly employ positive selection (PS) and negative selection (NS) algorithms, along with a clonal selection (CS) process wherein B lymphocytes generate more potent antibodies to combat antigens effectively. PS and NS algorithms distinguish self from non-self, while the CS process enhances antibody effectiveness [37].

The initialization step involves normalizing training data and measuring distance and affinity [38]. Accurate class labeling and normalization of training data to a range of [0, 1] simplify distance calculations between data dimensions. Affinity is calculated using normalized data through Euclidean distance in the antigen training process. Establishing a pool of memory cells, representing training data exemplars, is crucial for successful classification based on the AIS algorithm. Hence, initializing data and system variables for model training is pivotal. During antigen training, recognition cells in the memory pool respond to antigens, with each cell allocated a stimulation value inversely proportional to affinity. The memory cell with the highest stimulation is selected as the best match in subsequent memory cell selection steps. Subsequently, the classification process distinguishes between normal and faulty data.

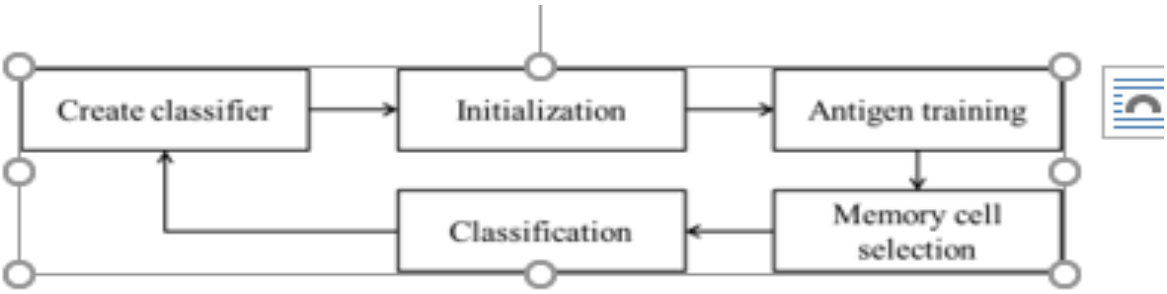

Figure 1. Overview of the artificial immune system (AIS) algorithm.

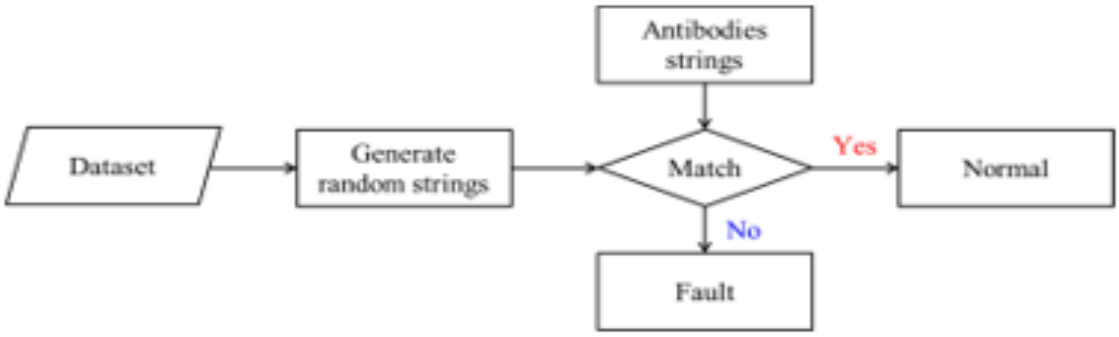

Figure 2. Classification using the negative selection (NS) algorithm flowchart.

As depicted in Figure 2, the negative selection (NS) algorithm comprises two main steps: the generation of random strings and the matching process. In the random string step, random antibodies are generated, and each sample from the training set is compared to the "self" sample represented by the antibody strings. During the matching step, if an antibody categorizes the sample as belonging to the "self" class, indicative of the normal state, the antibody is discarded from the antibody population. Consequently, if the Euclidean distance between the newly introduced data and the trained data is similar (termed as a match in the AIS algorithm), it is deemed as "self," representing the normal state. Conversely, if there is dissimilarity, it is categorized as "non-self," indicating an abnormal state [39]. In this study, data failing to match are classified as faulty data.

Table 1 provides explanations of the abbreviations used in the pseudo code, while Algorithm 1 presents the pseudo code for the initialization and antigen training steps. Within Algorithm 1, the "Calculate_affinity" function in the antigen training step computes the Euclidean distance between the selected memory cell representing the antibody string and the newly introduced data. It then verifies whether this calculated value aligns with existing data through the "distance_match" function. Algorithm 2 delineates the pseudo code for the classification method utilizing the NS

algorithm depicted in Figure 2. If the distance between the data to be predicted and the antibody serving as the detector does not match, it is classified as "non-self"; conversely, if it matches, it is classified as "self."

Table 1. Explanation of abbreviations used in pseudo code.

Abbreviation	Explanation
S_{self}	Sample of "self"
Population	Set of elements of S_{self}
$S_{antibodies}$	Set of antibodies that act as a detector
C_{normal}	Set of class of "normal" state
C_{fault}	Set of class of "fault" state
Self	Class predicted to be "normal" state
Non-self	Class predicted to be "fault" state

Algorithm 1. Pseudo Code for artificial immune system (AIS) training.

```
Initialization:
  Training set = normalize(training set)
Training:
  BEGIN
    Creation of self sample set (S_self)
    Population = {}
    WHILE for end of training
      antibody_new = generate_random_antibody()
      Calculate affinity
      distance_match = FALSE
      FOR EACH s = { s|s ∈ S_self }
        IF match (s, antibody_new)
          match = TRUE
        ELSE
          population += s
        END IF
      END FOR EACH
    END WHILE
  END
```

Algorithm 2. Pseudo Code for artificial immune system (AIS) classification.

```
BEGIN
  Creation of antibodies set by training algorithm (S_antibodies)
  FOR EACH detectors = { s|s ∈ S_antibodies (s) }
    IF NOT distance_match (s, C_self)
      Return 'non-self'
    ENDIF
  END FOR EACH
  RETURN 'self'
END
```

The AIS algorithm embodies several key characteristics: self-regulation, high performance, parameter stability, and the necessity of labeling [40]. Self-regulation eliminates the need for manual selection of the algorithm's internal structure; instead, the algorithm autonomously discovers and learns the appropriate structure during model training. Compared to other classification systems, the AIS algorithm demonstrates notably high accuracy even with limited data. Its efficiency lies in its ability to rapidly train models, as it operates as a single-shot detection algorithm. This

swiftness, combined with its capacity to identify optimal parameter values, ensures parameter stability. Furthermore, the algorithm's adeptness at achieving optimal results across a broad parameter spectrum facilitates effective tuning techniques for enhanced outcomes. Despite potentially requiring extensive labeling efforts in the training dataset for antigen definition, the AIS algorithm's ability to swiftly and accurately differentiate between normal and faulty conditions is paramount. These inherent features and classification capabilities enable the creation of a population of straightforward classifiers.

In this study, we implemented an AIS algorithm for real-time anomaly detection in semiconductor manufacturing equipment. The dataset was generated through deliberate modifications of gas supply parameter settings, capitalizing on the NS algorithm's innate ability to self-identify foreign substances.

Experiment and Data Acquisition:

Semiconductor equipment comprises multiple system modules, including RF power, process, and gas delivery, each consisting of numerous submodules and parts [25]. Over time, these parts degrade and may malfunction, affecting the overall performance of the equipment. Plasma etch process equipment is particularly sensitive to various parameters, with the gas flow rate through a mass flow controller (MFC) directly influencing the chemical reactions within the plasma, thereby influencing the etch profile and selectivity. In this study, our focus was on the performance degradation of MFCs within the plasma etch system.

Experimental data were acquired through a carefully designed scenario simulating the degradation of MFCs, which regulate the gas flow rate through the process chambers [41]. We utilized a 300-mm plasma etch system featuring 13.56-MHz RF-powered inductively coupled plasma-reactive ion etching (ICP-RIE) for the experiment. Experimental runs were conducted under conditions where the MFC controlling the flow of SF6 gas was intentionally degraded during anisotropic silicon trench etching using a mixture of SF6, O2, and Ar over time. To mimic the malfunction scenario, we deliberately adjusted the set value of the SF6 MFC by 2 standard cubic centimeters per minute (sccm), assuming that the parameter set point remained unchanged. In essence, although the actual amount of injected gas deviated from the prescribed recipe during steady-state operation, it was assumed that neither the MFC nor the

equipment could properly recognize this deviation on their own. Table 2 outlines the process recipe for the experimental conditions.

Table 2. Best-known method (BKM) process recipe.

Experiment Condition	Value
Pressure (mTorr)	20
Source power (W)	800
Bias power (W)	50
SF_6 gas flow rate (sccm)	158–194
O_2 gas flow rate (sccm)	124
Ar gas flow rate (sccm)	10
Chuck Temperature (°C)	25
Time (s)	180

Collecting and monitoring SVID data in real-time is imperative during the experiment, as even slight drifts in its value can have significant implications due to the process's high sensitivity to plasma dynamics. The plasma is profoundly influenced by process recipe parameters such as bias power and gas flow rate during its formation. To facilitate real-time acquisition of SVID data from semiconductor manufacturing equipment, we utilized High-speed SECS Message Service (HSMS) communication in conjunction with MariaDB. Figure 3 illustrates the overall data flow.

HSMS serves as a standard transport communication protocol in semiconductor factories, offering a Transmission Control Protocol/Internet Protocol (TCP/IP)-based Ethernet connection alternative to the simple SECS-I protocol, as per SEMI standards [42]. Through HSMS communication, a larger volume of data can be efficiently obtained using the faster TCP/IP protocol over Ethernet, as opposed to the RS-232 communication method. Moreover, it offers the advantage of easy hardware configuration, requiring only a local area network (LAN) environment. We developed the HSMS communication program using Visual Basic, with the communication connection state diagram depicted in Figure 4. Table 3 outlines the connection method.

The red dot in Figure 4 indicates the initial communication status. If there is no TCP/IP connection to the equipment, the process begins at the red dot before number 1; however, if a connection is established, it initiates from the dot within the connected status box. Following confirmation of the connection through the Stream 1 Function1 (S1F1) command, communication between the server computer and the semiconductor equipment commences via the S2F23 command, with transaction messages, i.e., SVID data values, received through S6F1. The communication connection

state must be in the "HSMS established selected" state to receive data. Through the program, SVID and OES data, representing two data types, were simultaneously collected at 1-second intervals from the described faulty process scenario involving intentional modifications of the gas flow rate in the system employed in this research.

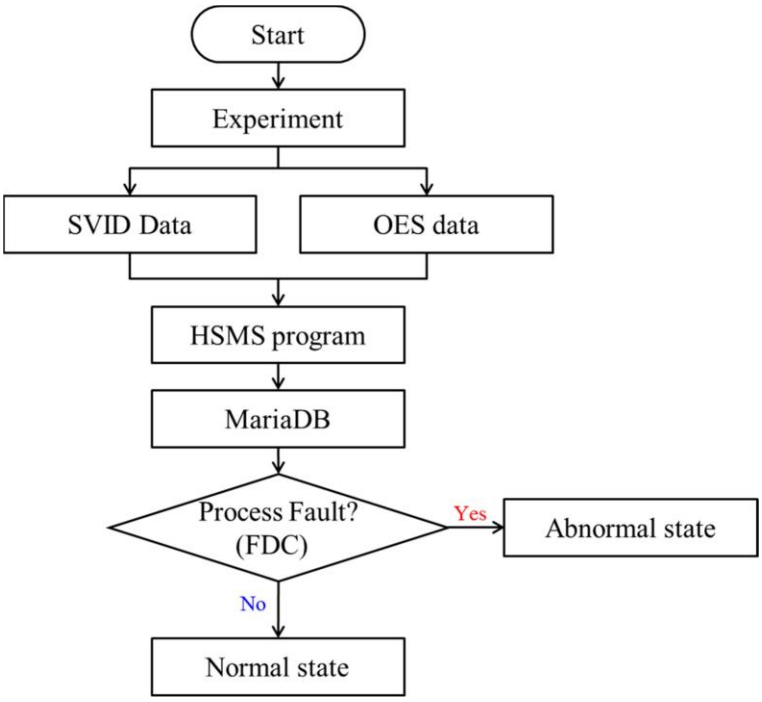

Figure 3. Data monitoring and acquisition system. State variable identification (SVID), High- speed SECS Message Service (HSMS), optical emission spectroscopy (OES), fault detection and classification (FDC).

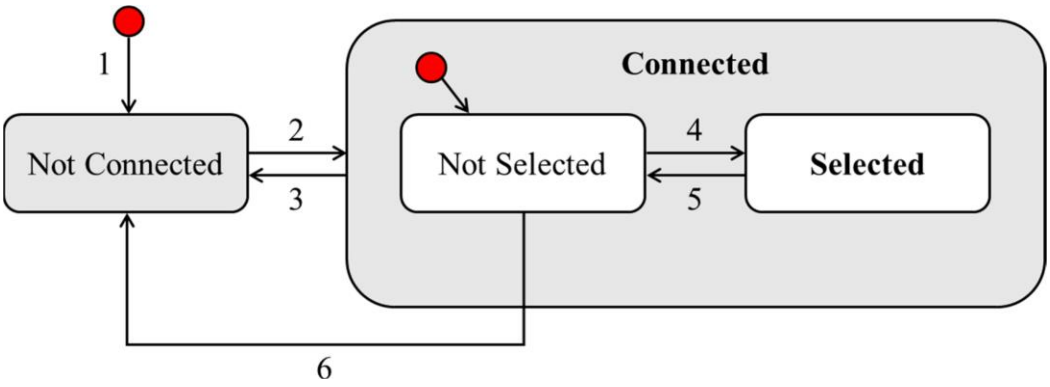

Figure 4. High-speed SECS message service (HSMS) communication connection state diagram.

Modeling and Results:

Intentionally modifying the gas flow rate during the experiment demonstrated its significant influence on the plasma and process outcomes. The etch rate trend, as well as OES intensities and SF6 gas flow rate variations, were observed to correspond to the specific faulty process scenario under consideration. Figure 5 depicts cross-sectional scanning electron microscope (SEM) images illustrating the SF6 gas amount increasing to (a) 174, (b) 176, (c) 188, and (d) 190 standard cubic centimeters per minute (sccm). Although the results do not exhibit a perfectly linear relationship, a discernible trend emerges where the etch depth appears to decrease as the gas flow rate increases. This phenomenon arises from the heightened number of collisions in the plasma due to the increased presence of gas molecules within a given pressure. OES data further corroborate this hypothesis regarding collision dynamics.

Figure 6 presents three selected wavelengths out of eight OES data sets: 705 nm for fluorine (F), 779 nm for oxygen (O), and 357 nm for argon (Ar). Interestingly, the SF6 gas flow rate and OES intensity demonstrate an inverse relationship. In plasma, electrons are generated through collisions, and plasma glow discharge occurs when energetically excited electrons dissipate their energy. It is inferred that the augmented gas flow contributed to an increased collisional cross-section within the plasma, thereby leading to heightened OES intensities at the corresponding wavelength peaks.

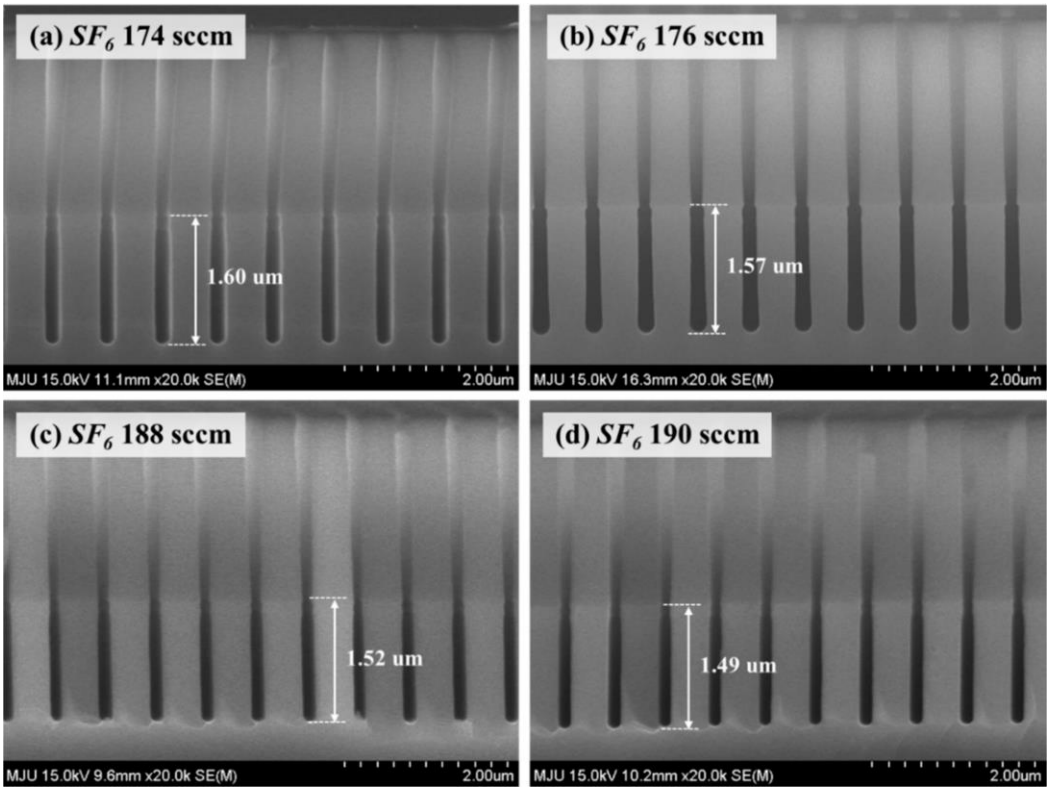

Figure 5. Cross-sectional scanning electron microscope (SEM) images depicting silicon etch profiles under varying SF6 gas flow rates: (a) 174 sccm, (b) 176 sccm, (c) 188 sccm, and (d) 190 sccm. Increasing gas flow rates resulted in reduced silicon etch depth, with image (b) displaying the most pronounced undesired etch profile featuring lateral sidewall etching.

Figure 6 illustrates the change in optical emission spectroscopy (OES) intensity alongside the SF6 gas flow rate across

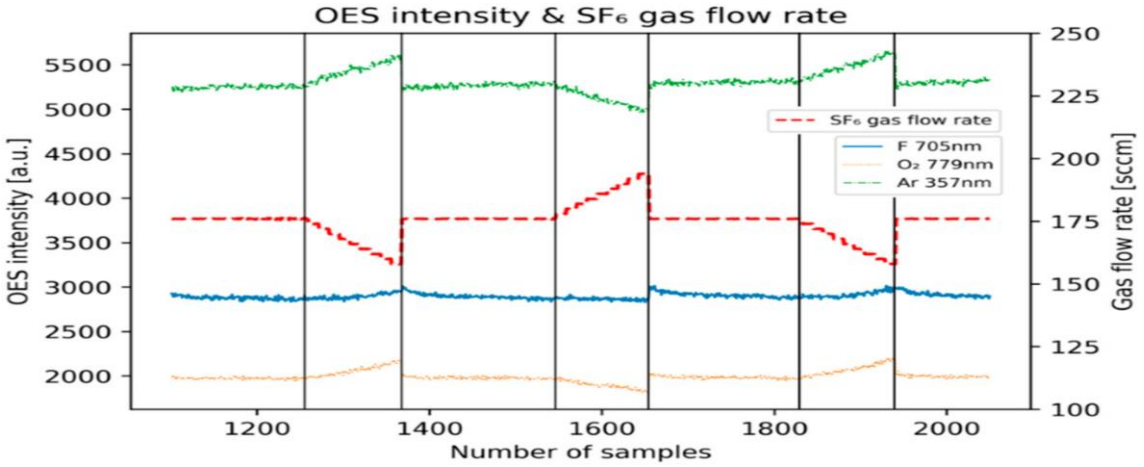

the faulty process scenario.

We observed a decrease in OES intensity with increasing gas flow rate, a phenomenon attributed to the negative ionization tendency of SF6 gas. Upon ionization, SF6 generates F radicals, which exhibit a strong negative ionization tendency and effectively trap free electrons in their vicinity. This phenomenon is similarly observed with O2, which also possesses a strong negative ionization tendency. Consequently, the abundance of free electrons diminishes significantly, leading to a decrease in the number of excited electrons [44].

Conversely, a decrease in gas flow rate results in an increase in OES intensity, following the same principle. Ultimately, the variation in gas flow rate induces changes in the plasma dynamics, manifesting as alterations in OES intensity and etch depth, as summarized in Table 6.

Table 6. Phenomenon by changes in SF_6 gas flow rate.

	Etch Depth	OES Intensity
SF_6 gas flow rate↑	↓	↓
SF_6 gas flow rate↓	↑	↑

Modeling and Results:

We conducted two modeling cases utilizing different input data sets: (1) SVID equipment data combined with selected OES data, and (2) selected OES data alone. In the first case, we incorporated SVID 434, SVID 440, and SVID 491 representing real gas flow rate values, along with eight OES data sets featuring different wavelength intensities (as detailed in Table 5). These inputs were then compared with the modeling results obtained using only the selected OES data.

The model predictions regarding the equipment's normal state are as follows. The prediction accuracy for both modeling cases, utilizing selected SVID and OES data and OES data alone, stands at 94.69% and 93.68%, respectively. Despite the simulated minute process shifts, where the set value of the gas flow rate was altered by 2 sccm and the real injected gas value fluctuated by 1 sccm, both models demonstrated high classification accuracies. Our findings suggest that while it is feasible to incorporate real gas flow rate values into the model, a simulated experiment using solely OES data suffices for MFC failure detection. The simulated increase in SF6 gas flow leads to corresponding changes in OES data. As SF6 gas flow rises, the presence of O2 in the chamber increases, elevating the ratio of O2 in the total gas. Since O2 gas exhibits lower electronegativity than SF6 gas, an increase in O2 content boosts electron density [45]. Consequently, the rise in O2 content enhances F radical concentrations related to Si etching, thereby increasing the etch rate, as depicted in Figure 5 [46]. Figures 6–8 further illustrate the variations in F (703 nm) and O (777 nm) observed in the fault data, where SF6 gas flow is manipulated. These results underscore the utility of OES for real-time equipment fault diagnosis, particularly for gas-related faults.

It is important to emphasize that the aim of this study is to detect unnoticed equipment faults and classify their causes. We demonstrated fault detection and classification (FDC) with respect to gas flow rate variations. The prediction accuracies of the two models are summarized in Table 7. To visually represent the classification results of the two models in two dimensions, the classification predictions based on two inputs from the eight OES wavelength data sets are illustrated in Figure 7. Specifically, Figures 7a and 7b depict the classification results of the model utilizing both SVID and OES data, while Figures 7c and 7d display the classification results of the model using only OES data. Furthermore, in Figures 7b and 7d, the prediction accuracy is elaborated by adding labels to the figures. When the model correctly predicts the process result state as normal, it is denoted as "T_normal" for true normal and "F_normal" for false normal when it is actually in an abnormal state. Similarly, if the model accurately predicts the process result

state as abnormal, it is indicated as "T_abnormal"; otherwise, it is labeled as "F_abnormal." Finally, Figure 8 illustrates the effective classification of high-dimensional data through 3D plotting.

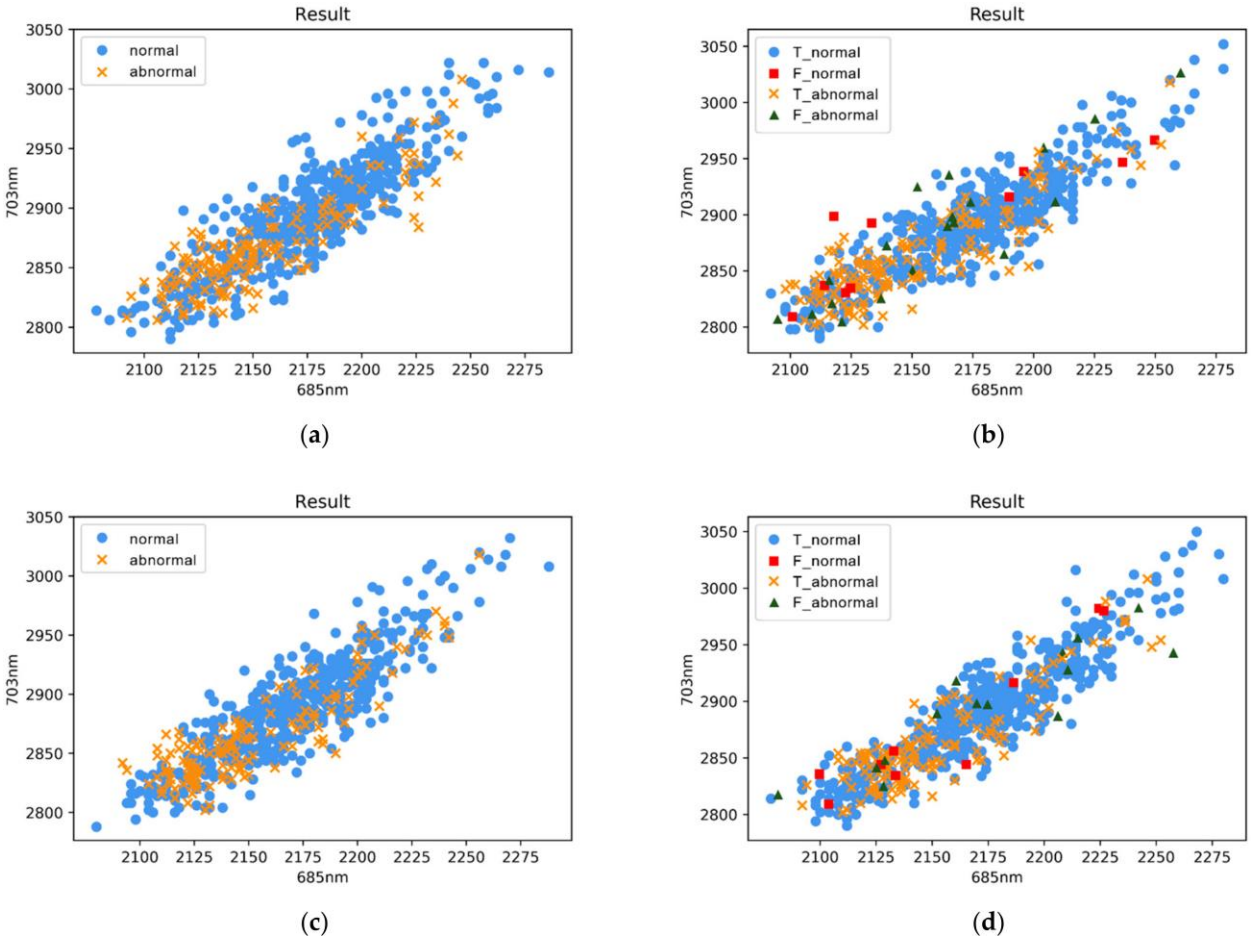

Figure 7. 2D plotting of modeling classification results: with state variable identification (SVID) and optical emissionspectroscopy (OES) data of (**a**) train data and (**b**) test data; with only OES data of (**c**) train data and (**d**) test data.

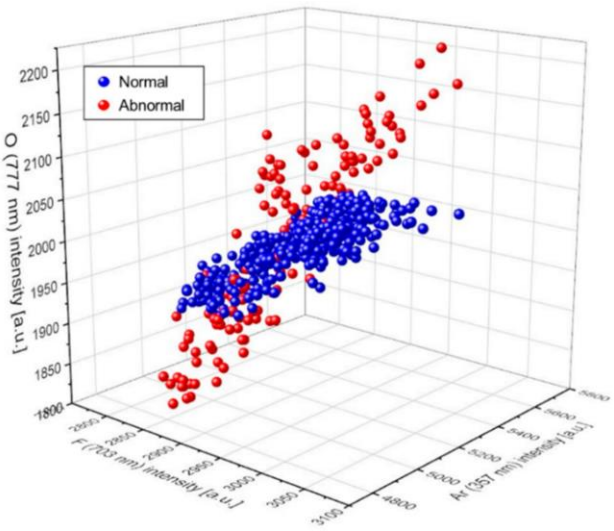

Table 7. Model prediction accuracy results. The unit is %. State variable identification (SVID), optical emission spectroscopy (OES).

Data Type	Total	Train	Test
SVID and OES data	94.69	95.12	94.52
OES data only	93.68	94.20	93.36

As a result, we have validated the potential application of a novel Fault Detection and Classification (FDC) methodology utilizing the AIS algorithm for equipment abnormality detection. Furthermore, we have established that the abnormal state can be effectively identified using only Optical Emission Spectroscopy (OES) data, which reflects real-time plasma conditions, achieving similar accuracy to the modeling results obtained with the inclusion of both SVID and OES data, encompassing actual gas flow rate values.

Conclusions

This research introduces a real-time FDC approach for semiconductor etch processes leveraging AIS algorithms, inspired by immunological response systems. Section 3 outlines the AIS algorithm proposed for FDC, while Section 4 details the experimental setup involving intentional modification of gas flow rates and the acquisition of two types of data for modeling. In Section 5, we demonstrated the impact of SF6 gas flow rate variations on plasma dynamics and FDC using the AIS algorithm. Consequently, modeling accuracy using selected SVID and OES data reached

94.69%, with 93.68% accuracy obtained solely from OES data. Both models effectively classified high-dimensional data with high accuracy.

Moreover, unlike conventional machine learning-based approaches for FDC, the AIS algorithm exhibits self-regulation, obviating the need for hyperparameter optimization. Even with a modest dataset of 2408 samples, the AIS algorithm facilitated learning and prediction without overfitting. While labeled training data were employed for accurate learning in this study, the AIS algorithm's inherent capacity for unsupervised learning remains untapped. Furthermore, our FDC methodology, although focused on the aging of a single part, lays the groundwork for future investigations into identifying and detecting faults across the diverse components comprising semiconductor equipment. Subsequent experiments simulating aging in various equipment parts are recommended.

In conclusion, our findings demonstrate that MFC aging-induced abnormal states can be effectively detected by monitoring plasma conditions based on OES data, facilitated by the novel FDC methodology employing AIS algorithms. Analogous to the human body's immune system detecting and responding to foreign invaders such as viruses, our FDC methodology equipped with AIS algorithms swiftly identifies equipment abnormalities based on OES plasma monitoring data.

References:

[1]. Maharjan, R., Chy, M. S. H., Arju, M. A., & Cerny, T. (2023, June). Benchmarking Message Queues. In *Telecom* (Vol. 4, No. 2, pp. 298-312). MDPI. https://doi.org/10.3390/telecom4020018

[2]. Chy, M. S. H., Arju, M. A. R., Tella, S. M., & Cerny, T. (2023). Comparative Evaluation of Java Virtual Machine-Based Message Queue Services: A Study on Kafka, Artemis, Pulsar, and RocketMQ. *Electronics*, *12*(23), 4792. https://doi.org/10.3390/electronics12234792

[3]. Rahman, M., Chy, M. S. H., & Saha, S. (2023, August). A Systematic Review on Software Design Patterns in Today's Perspective. In *2023 IEEE 11th International Conference on Serious*

Games and Applications for Health (SeGAH) (pp. 1-8). IEEE. https://doi.org/10.1109/SeGAH57547.2023.10253758

[4]. Shivakumar, S. K., & Sethii, S. (2019). *Building Digital Experience Platforms: A Guide to Developing Next-Generation Enterprise Applications*. Apress.

[6]. Sethi, P. Karmuru, & Tayal.(2023). Analyzing and Designing a Full-Text Enterprise Search Engine for Data-Intensive Applications. *International Journal of Science, Engineering and Technology, 11*. https://www.ijset.in/wp-content/uploads/IJSET_V11_issue6_628.pdf

[7]. Sethi, S., Panda, S., & Kamuru, R. (2023). Comparative study of middle tier caching solution. *International Journal of Development Research*, *13*(11), 64225-64229.

[8]. Gitte, M., Bawaskar, H., Sethi, S., & Shinde, A. (2014). Content based video retrieval system. *International Journal of Research in Engineering and Technology*, *3*(06), 123-129.

[9]. Gitte, M., Bawaskar, H., Sethi, S., & Shinde, A. (2014). Content based video retrieval system. *International Journal of Research in Engineering and Technology*, *3*(06), 123-129.

[10]. Sethi, S., & Shivakumar, S. K. (2023). DXPs Digital Experience Platforms Transforming Fintech Applications: Revolutionizing Customer Engagement and Financial Services. *International Journal of Advance Research, Ideas and Innovations in Technology*, *9*, 419-423.

[11]. Jhurani, J. REVOLUTIONIZING ENTERPRISE RESOURCE PLANNING: THE IMPACT OF ARTIFICIAL INTELLIGENCE ON EFFICIENCY AND DECISION-MAKING FOR CORPORATE STRATEGIES.

[12]. Jhurani, J. Enhancing Customer Relationship Management in ERP Systems through AI: Personalized Interactions, Predictive Modeling, and Service Automation.

[13]. Jhurani, J. DRIVING ECONOMIC EFFICIENCY AND INNOVATION: THE IMPACT OF WORKDAY FINANCIALS IN CLOUD-BASED ERP ADOPTION.

[14]. Smith, J. D. Influence of Self-Efficacy, Stress, and Culture on the Productivity of Industrial Sales Executives in Latin American Sales Networks.

[15]. Miah, S., Rahaman, M. H., Saha, S., Khan, M. A. T., Islam, M. A., Islam, M. N., ... & Ahsan, M. H. (2013). Study of the internal structure of electronic components RAM DDR-2 and motherboard of nokia-3120 by using neutron radiography technique. *International Journal of Modern Engineering Research (IJMER)*, *3*(60), 3429-3432

[16]. Rahaman, M. H., Faruque, S. B., Khan, M. A. T., Miah, S., & Islam, M. A. (2013). Comparison of General Relativity and Brans-Dicke Theory using Gravitomagnetic clock effect. *International Journal of Modern Engineering Research*, *3*, 3517-3520.

[17]. Miah, M. H., & Miah, S. (2015). The Investigation of the Effects of Blackberry Dye as a Sensitizer in TiO2 Nano Particle Based Dye Sensitized Solar Cell. *Asian Journal of Applied Sciences*, *3*(4).

[18]. Miah, S., Miah, M. H., Hossain, M. S., & Ahsan, M. H. (2018). Study of the Homogeneity of Glass Fiber Reinforced Polymer Composite by using Neutron Radiography. *Am. J. Constr. Build. Mater*, *2*, 22-28.

[19]. Miah, S., Islam, G. J., Das, S. K., Islam, S., Islam, M., & Islam, K. K. (2019). Internet of Things (IoT) based automatic electrical energy meter billing system. *IOSR Journal of Electronics and Communication Engineering*, *14*(4 (I)), 39-50.

[20]. Nadia, A., Hossain, M. S., Hasan, M. M., Islam, K. Z., & Miah, S. (2021). Quantifying TRM by modified DCQ load flow method. *European Journal of Electrical Engineering*, *23*(2), 157-163.

[21]. Miah, S., Raihan, S. R., Sagor, M. M. H., Hasan, M. M., Talukdar, D., Sajib, S., ... & Suaiba, U. (2022). Rooftop Garden and Lighting Automation by the Internet of Things (IoT). *European Journal of Engineering and Technology Research*, *7*(1), 37-43.

DOI: https://doi.org/10.24018/ejeng.2022.7.1.2700

[22]. Prasad, A. B., Singh, S., Miah, S., Singh, A., & Gonzales-Yanac, T. A Comparative Study on Effects of Work Culture on employee satisfaction in Public & Private Sector Bank with special reference to SBI and ICICI Bank.

[23]. Ravichandra, T. (2022). A Study On Women Empowerment Of Self-Help Group With Reference To Indian Context.https://www.webology.org/data-cms/articles/20220203075142pmwebology%2019%20(1)%20-%2053.pdf

[24]. Kumar, H., Aoudni, Y., Ortiz, G. G. R., Jindal, L., Miah, S., & Tripathi, R. (2022). Light weighted CNN model to detect DDoS attack over distributed scenario. *Security and Communication Networks*, *2022*. https://doi.org/10.1155/2022/7585457

[25]. Ma, R., Kareem, S. W., Kalra, A., Doewes, R. I., Kumar, P., & Miah, S. (2022). Optimization of electric automation control model based on artificial intelligence algorithm. *Wireless Communications and Mobile Computing*, *2022*. https://doi.org/10.1155/2022/7762493

[26]. Devi, O. R., Webber, J., Mehbodniya, A., Chaitanya, M., Jawarkar, P. S., Soni, M., & Miah, S. (2022). The Future Development Direction of Cloud-Associated Edge-Computing Security in the Era of 5G as Edge Intelligence. *Scientific Programming*, *2022*. https://doi.org/10.1155/2022/1473901

[27]. Al Noman, M. A., Zhai, L., Almukhtar, F. H., Rahaman, M. F., Omarov, B., Ray, S., ... & Wang, C. (2023). A computer vision-based lane detection technique using gradient threshold and hue-lightness-saturation value for an autonomous vehicle. *International Journal of Electrical and Computer Engineering*, *13*(1), 347.

[28]. Patidar, M., Shrivastava, A., Miah, S., Kumar, Y., & Sivaraman, A. K. (2022). An energy efficient high-speed quantum-dot based full adder design and parity gate for nano application. *Materials Today: Proceedings*, *62*, 4880-4890.https://doi.org/10.1016/j.matpr.2022.03.532

[29]. Pillai, A. S. (2023). Advancements in Natural Language Processing for Automotive Virtual Assistants Enhancing User Experience and Safety. *Journal of Computational Intelligence and Robotics*, *3*(1), 27-36.

[30]. Rahman, S., Mursal, S. N. F., Latif, M. A., Mushtaq, Z., Irfan, M., & Waqar, A. (2023, November). Enhancing Network Intrusion Detection Using Effective Stacking of Ensemble Classifiers With Multi-Pronged Feature Selection Technique. In *2023 2nd International Conference on Emerging Trends in Electrical, Control, and Telecommunication Engineering (ETECTE)* (pp. 1-6). IEEE. https://doi.org/10.1109/ETECTE59617.2023.10396717

[31]. Latif, M. A., Afshan, N., Mushtaq, Z., Khan, N. A., Irfan, M., Nowakowski, G., ... & Telenyk, S. (2023). Enhanced classification of coffee leaf biotic stress by synergizing feature concatenation and dimensionality reduction. *IEEE Access*. https://doi.org/10.1109/ACCESS.2023.3314590

[32]. Irfan, M., Mushtaq, Z., Khan, N. A., Mursal, S. N. F., Rahman, S., Magzoub, M. A., ... & Abbas, G. (2023). A Scalo gram-based CNN ensemble method with density-aware smote oversampling for improving bearing fault diagnosis. *IEEE Access*, *11*, 127783-127799. https://doi.org/10.1109/ACCESS.2023.3332243

[33]. Irfan, M., Mushtaq, Z., Khan, N. A., Althobiani, F., Mursal, S. N. F., Rahman, S., ... & Khan, I. (2023). Improving Bearing Fault Identification by Using Novel Hybrid Involution-Convolution Feature Extraction with Adversarial Noise Injection in Conditional GANs. *IEEE Access*. https://doi.org/10.1109/ACCESS.2023.3326367

[34]. Latif, M. A., Mushtaq, Z., Arif, S., Rehman, S., Qureshi, M. F., Samee, N. A., ... & Al-masni, M. A. Improving Thyroid Disorder Diagnosis via Ensemble Stacking and Bidirectional Feature Selection. https://www.techscience.com/cmc/v78n3/55928/html

[35]. Gunasekaran, K. P., Babrich, B. C., Shirodkar, S., & Hwang, H. (2023, August). Text2Time: Transformer-based Article Time Period Prediction. In *2023 IEEE 6th International Conference on Pattern Recognition and Artificial Intelligence (PRAI)* (pp. 449-455). IEEE. https://doi.org/10.1109/PRAI59366.2023.10331985

[36]. Gunasekaran, K., & Jaiman, N. (2023, August). Now you see me: Robust approach to partial occlusions. In *2023 IEEE 4th International Conference on Pattern Recognition and*

Machine Learning (PRML) (pp. 168-175). IEEE. https://doi.org/10.1109/PRML59573.2023.10348337

[37]. Kommaraju, V., Gunasekaran, K., Li, K., Bansal, T., McCallum, A., Williams, I., & Istrate, A. M. (2020). Unsupervised pre-training for biomedical question answering. *arXiv preprint arXiv:2009.12952*. https://doi.org/10.48550/arXiv.2009.12952

[38]. Bansal, T., Gunasekaran, K., Wang, T., Munkhdalai, T., & McCallum, A. (2021). Diverse distributions of self-supervised tasks for meta-learning in NLP. *arXiv preprint arXiv:2111.01322*. https://doi.org/10.48550/arXiv.2111.01322

[39]. Mahalingam, H., Velupillai Meikandan, P., Thenmozhi, K., Moria, K. M., Lakshmi, C., Chidambaram, N., & Amirtharajan, R. (2023). Neural attractor-based adaptive key generator with DNA-coded security and privacy framework for multimedia data in cloud environments. *Mathematics*, *11*(8), 1769. https://doi.org/10.3390/math11081769

[40]. Padmapriya, V. M. (2018). Image transmission in 4g lte using dwt based sc-fdma system. *Biomedical & Pharmacology Journal*, *11*(3), 1633. https://dx.doi.org/10.13005/bpj/1531

[41]. Padmapriya, V. M., Thenmozhi, K., Praveenkumar, P., & Amirtharajan, R. (2020). ECC joins first time with SC-FDMA for Mission “security”. *Multimedia Tools and Applications*, *79*(25), 17945-17967. https://doi.org/10.1007/s11042-020-08610-5

[42]. Padmapriya, V. M., Sowmya, B., Sumanjali, M., & Jayapalan, A. (2019, March). Chaotic Encryption based secure Transmission. In *2019 International Conference on Vision Towards Emerging Trends in Communication and Networking (ViTECoN)* (pp. 1-5). IEEE. https://doi.org/10.1109/ViTECoN.2019.8899588

[43]. Padmapriya, V. M., Thenmozhi, K., Praveenkumar, P., & Amirtharajan, R. (2022). Misconstrued voice on SC-FDMA for secured comprehension-a cooperative influence of DWT and ECC. *Multimedia Tools and Applications*, *81*(5), 7201-7217. https://doi.org/10.1007/s11042-022-11996-z

[44]. Padmapriya, V. M., Thenmozhi, K., Avila, J., Amirtharajan, R., & Praveenkumar, P. (2020). Real Time Authenticated Spectrum Access and Encrypted Image Transmission via Cloud Enabled Fusion centre. *Wireless Personal Communications*, *115*, 2127-2148. https://doi.org/10.1007/s11277-020-07674-8

[45]. Padmapriya, V. M., Priyanka, M., Shruthy, K. S., Shanmukh, S., Thenmozhi, K., & Amirtharajan, R. (2019, March). Chaos aided audio secure communication over SC-FDMA system. In *2019 International Conference on Vision Towards Emerging Trends in Communication and Networking (ViTECoN)* (pp. 1-5). IEEE. https://doi.org/10.1109/ViTECoN.2019.8899413